昭和62年8月5日第三種郵便物許可　令和３年10月25日発行（隔月25日発行）　第39巻　第５号

MATERIAL TECHNOLOGY

材料技術

September-October

2021

Vol. 39, No. 5

ISSN 0289-7709

CODEN: MTECFQ

材料技術研究協会

Japan Research Institute of
Material Technology

https://www.jrimt.jp

MATERIAL
TECHNOLOGY
材料技術

VOL. 39, NO. 5
September-October

Contents

Chalcone (1,3-diphenyl-2-propen-1-one) induces apoptosis of HeLa CD4$^+$ cells through caspase signaling pathways

Rumiko SAITO [1)], Kahoko HASHIMOTO [1)], and Naoko MIYAMO-KUROSAKI [1)] *

Abstract

Chalcone (1,3-diphenyl-2-propen-1-one), a precursor of all flavonoids, is distributed widely among higher plants, and chalcone derivatives have been reported to exhibit antitumor activity *in vitro* as well as *in vivo*. However, few reports have detailed the mechanism through which chalcone induces apoptosis. Thus, this study was undertaken to investigate the apoptotic effect of chalcone on cervical cancer cells *in vitro*. The effect of chalcone on HeLa CD4$^+$ cell viability was evaluated with the CCK-8 assay, which revealed that chalcone can reduce the viability of HeLa CD4$^+$ cells. Morphological and biochemical assays, including phase contrast and PI staining fluorescence microscopy, were used to examine apoptosis induction. Both fluorescence and phase contrast microscopy showed that 24 h treatments with chalcone induced typical apoptotic features in HeLa CD4$^+$ cells, including chromatin condensation, DNA fragmentation, and apoptotic body formation. Annexin V/PI assays were performed using flow cytometry to quantitatively test the effect of chalcone on apoptosis, revealing that chalcone induced apoptosis of HeLa CD4$^+$cells. Finally, activity of caspase-8, -9, and -3 was induced by chalcone treatment, indicating that chalcone induces apoptosis of HeLa CD4$^+$ cells via the caspase signaling pathway.

Keywords：Chalcone (1,3-diphenyl-2-propen-1-one), Apoptosis, HeLa CD4$^+$ cells

Received September 19, 2021; accepted October 11, 2021

1) Department of Life and Environmental Sciences, Graduate School of Engineering, Chiba Institute of Technology, 2-17-1 Tsudanuma, Narashino, Chiba 275-0016, Japan

*Corresponding author: Naoko Miyano-Kurosaki, Department of Life and Environmental Sciences, Graduate School of Engineering, Chiba Institute of Technology, 2-17-1 Tsudanuma, Narashino, Chiba 275-0016, Japan

E-mail: kurosaki.naoko@p.chibakoudai.jp

1 Introduction

In 2018, there were an estimated 569,800 new cases of and 311,400 deaths caused by cervical cancer worldwide[1,2] . Cervical cancer is both the third most frequently diagnosed cancer and the third leading cause of cancer-related deaths following breast and lung cancers[2] . Treatments for cervical cancer include surgery, radiation therapy, and chemotherapy (i.e., anticancer drug treatment)[3,4] . However, many of those treatments have serious side effects and negatively affect quality of life (QOL)[5] .

Many plants have antitumor pharmacological effects, and about two thirds of current anticancer agents, including Topotecan, Etoposide, and Paclitaxel, are compounds originally isolated from plants[6] . Some flavonoid compounds found among various foods and herbal medicines have anti-tumor effects[7,8] with fewer side effects[9,10] . For example, the naturally occurring chalcones 4-hydroxyderricin, xanthoangelol, and ashitaba chalcone isolated from the roots of *Angelica keiskei* (Miq.) Koidz (Umbelliferae) showed antitumor activity[11] . In Japan, the aboveground portions of this plant are consumed as food[12]. The basic structure of ashitaba chalcone (1,3-diphenyl-2-propen-1-one) is among the most important classes of flavonoids found throughout the whole plant kingdom[13] . Collectively, chalcones are an important group of polyphenols that can be isolated from a wide range of foods, including spices, fruits, teas, vegetables, and even beer[14,15] . Chalcones are open-chain precursors involved in flavonoid and isoflavonoid biosynthesis, and they occur mainly as polyphenol compounds that change from yellow to orange in color[13] . The chemical structure of 1,3-diaryl-2-propen-1-one consists of two aromatic rings linked by a 3-carbon α, β-unsaturated carbonyl system[16] . Multiple reports have detailed the antitumor effects of the many types of natural and synthetic chalcones. The biologically active properties of natural chalcones, which are mainly found in their hydroxyl form, have been reported previously[14,17] . Xanthoangelol, a natural chalcone, has been reported to both inhibit tumor promotion and metastasis as well as induce apoptosis in several cancer cell lines[18,19] . Similarly, isoliquiritigenin and licochalcone A have been demonstrated to arrest the cell cycle and induce apoptosis in various cancer cells[20,21] . The synthetic chalcone naphthylchalcone ((2E)-1-(3,4,5-trimethoxy-phenyl)-3-(1-naphthyl)-2-propene-1-one) has been found to induce apoptosis and block cell cycle progression by triggering both intrinsic and extrinsic pathways against hematologic malignancy cells[22] . Similarly, synthetic chalcone (2,3,4′-trimethoxy-2′-hydroxy-chalcone) induced apoptosis in human hepatocellular carcinoma cells through a caspase-dependent intrinsic pathway[23] . Butein has been reported to suppress cervical cancer via the PI3K/AKT/mTOR pathway[24] . In contrast, an analysis of the central structure of chalcone suggests that initiation may be involved in the antiproliferative activity of chalcone in which apoptosis is induced through mitochondrial and death receptor pathways in human breast cancer cells[25] . In human bladder cancer cells, chalcone has been shown to inhibit cell proliferation by inducing apoptosis and arresting cell cycle progression in the G2/M phase[26] .

The antitumor activity of chalcone in cervical cancer cells is associated with the cancer cell growth promoter tetradecanoylphorbol-13-acetate (TPA) in HeLa $CD4^+$ cells and its inhibitory activity against phosphorylation[12] . Chalcone has also been demonstrated to have chemopreventive effects through enhancement of the antitumor activity of TRAIL[27] .

However, the apoptotic pathway by which chalcone acts in cervical cancer cell HeLa $CD4^+$ cells is poorly understood. Accordingly, we aimed to elucidate the apoptotic pathway in which chalcone has antitumor activity against HeLa $CD4^+$ cells.

2 Experimental

2.1. Cells and reagents. HeLa cells stably transfected with human $CD4^+$ were generously supplied by Prof. Naoki Yamamoto (Tokyo Medical and Dental University). The cells were cultured at 37°C with a 5% CO_2 humidified atmosphere in Dulbecco's modified Eagle's medium (Sigma-Aldrich, St. Louis, MO) supplemented with 10% fetal bovine serum (Cytiva, Tokyo), 100 units/mL penicillin G and 100 μg/ml streptomycin (Fujifilm Wako Pure Chemical Corp, Osaka). Chalcone (1,3-diphenyl-2-propen-1-one, purity > 98.0%) was procured from Tokyo Chemical Industry Co., Ltd. (Tokyo) (Fig. 1A), and dimethyl sulfoxide (DMSO) was purchased from Fujifilm Wako Pure Chemical Corp (Osaka).

2.2. Cell viability assays. Cell viability was measured using cell counting kit-8 (CCK-8) (Dojindo Molecular Technologies, Inc., Kumamoto) in accordance with the manufacturer's instructions. In brief, in addition to negative control wells (without cells), 10^4 cells per well (in 100 μL of medium) were seeded into 96-well plates, with six replicate wells assigned to each group. After a 24 h incubation, the cells were treated with different doses of chalcone (0, 20, 40, 60, 80, or 100 μmol/L), and incubated again for 24 h, with 0.1% DMSO used as the vehicle. After adding 10 μL of CCK-8 solution to each well and incubating for 3 h in a dark incubator at 37°C, the 450 nm absorbance values (OD_{450} values) were measured using a microplate reader (Bio-Rad Laboratories, Hercules, CA) according to the manufacturer's instructions.

2.3. Cell cycle analysis. HeLa $CD4^+$ cells were seeded into 6-well cell culture plates (10^6 cells per well) and cultured for 24 h. Then, 50 μmol/L chalcone was added, and cells were harvested after another 24 h. Cells were afterwards washed with phosphate-buffered saline (PBS), fixed with 70% ethanol for 30 min at 4°C, and washed again with PBS containing 2% bovine serum albumin, after which 300 μL of PI / RNase Solution (Immunostep, Salamanca) was added to the resulting cell pellet. Following a 15 min incubation at room temperature, populations of PI-positive cells were analyzed with a BD FACSCalibur flow cytometer (BD Biosciences, Franklin Lakes, NJ). The experiment consisted of three or more independent replicates.

2.4. Assaying nuclear morphological changes by propidium iodide staining. The nuclear morphological changes caused by apoptosis were examined using propidium iodide staining 24 h after chalcone treatment. Briefly, 10^4 cells per well were seeded into 96-well plates. Following a 24 h incubation, the cells were treated with different doses of 50 μmol/L chalcone for 24 h, while the vehicle control used 0.1% DMSO instead. After treatment, cells were washed twice with 1× PBS and stained in darkness with 10 μg/mL propidium iodide (in PBS) for 10 min at room temperature. Cells were viewed at 515 nm under a fluorescent microscope (Keyence Co., Osaka,).

2.5. Apoptotic cell death detection by flow cytometry. An Annexin V-FITC apoptosis kit (Medical & Biological Laboratories Co., LTD., Tokyo) was used to identify phosphatidylserine externalization during the process of apoptosis, according to the manufacturer's instructions. Briefly, the HeLa $CD4^+$ cells (3×10^5 cells per well) were seeded into 6-well plates and incubated for 24 h prior to experimentation and then exposed to 50 μmol/L chalcone or 0.1% DMSO for 24 h. The cells were washed twice after the incubation, with PBS, and then resuspended in 42 μL of binding buffer. The resulting cell suspensions were incubated with 2.5 μL of propidium iodide and 5 μL of annexin V-FITC at room temperature in darkness for 15 min. Annexin V-positive cell populations were directly analyzed using BD FACSCalibur. The experiment was conducted with three or more independent replicates.

2.6. Caspase-8 and -9 activity assay. Caspase-8 and -9 activity was measured using Caspase-8 and -9 FITC staining kits, respectively (Abcam, Cambridge) according to the manufacturer's instructions. In brief, 10^6 cells were incubated in 6 cm dishes with 50 μmol/L chalcone. Caspase activity rates were analyzed using BD FACSCalibur. The experiment consisted of three or more independent replicates.

2.7. Caspase-3 activity assay. Caspase-3 activity was measured with the Caspase-3 (active) FITC staining kit (Abcam, Cambridge) according to the manufacturer's instructions. Briefly, 3×10^5 cells were incubated in 6-well plates with 50 μmol/L chalcone. Caspase activity rates were monitored using BD FACSCalibur. The experiment consisted of three or more independent replicates.

2.8 Statistical analysis. All data were processed using Microsoft Office Excel (Microsoft, Redmond, WA). All results are expressed as means ± standard deviation (SD) and each experiment was repeated independently at least 3 times. In addition, statistical differences were analyzed by Student's *t*-test. Statistical significance was indicated by $P < 0.05$ (both sides).

3 Result

3.1. Cytotoxic effects of chalcone inhibited HeLa CD4$^+$ cell growth. The effect of chalcone on HeLa CD4$^+$ cell viability was determined by treating the cells with various concentrations of chalcone (0 μmol/L to 100 μmol/L) for 24 h and evaluating subsequent cell viability using the CCK-8 assay (Fig. 1B). The addition of chalcone at various concentrations over 24 h affected HeLa CD4$^+$ cells, resulting in a concentration-dependent decrease in cell viability (Fig. 1B). After 24 h of chalcone treatment, up to 50% cell death was observed at a dose of 51.8 ± 4.3 μmol/L, and so subsequent experiments were performed with a chalcone addition of 50 μmol/L.

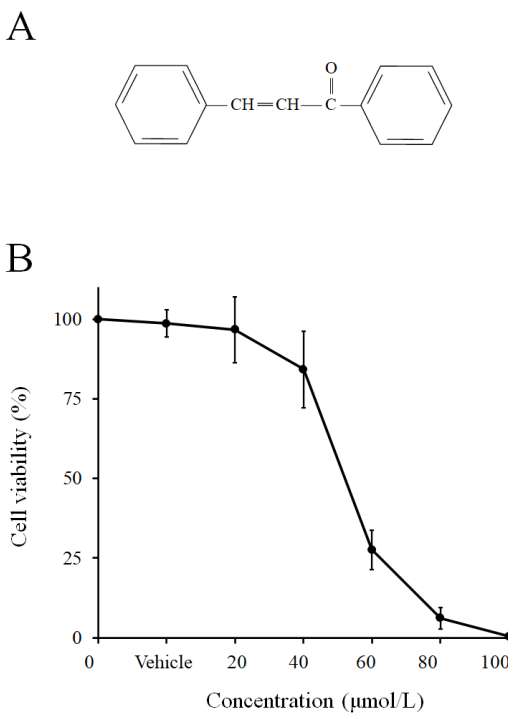

Fig 1. Inhibitory effect of chalcone on HeLa CD4$^+$ cell growth. (A) Chemical structure of 1,3-diphenyl-2-propen-1-one (chalcone); (B) Cell viability was determined by CCK-8 assay.

3.2. Chalcone increased the proportion of HeLa CD4$^+$ cells in sub-G1 phase. Flow cytometry was used to quantify cells in each cell cycle phase after the addition of chalcone. In the control, the percentage of HeLa CD4$^+$ cells in sub-G1 phase was 4.9 ± 0.5%. In contrast, the 24 h 50 μmol/L chalcone treatment significantly increased the percentage of cells in sub-G1 phase to 17.3 ± 1.0% (Fig. 2). The percentage of cells in the G0/G1 phase was significantly reduced from 53.6 ± 1.0% in the control to 42.1 ± 2.3% in the 24 h 50 μmol/L chalcone treatment (Fig. 2). For the other cell cycle phases, including the S phase and G2/M phase, the addition of chalcone did not significantly change in HeLa CD4$^+$ cells.

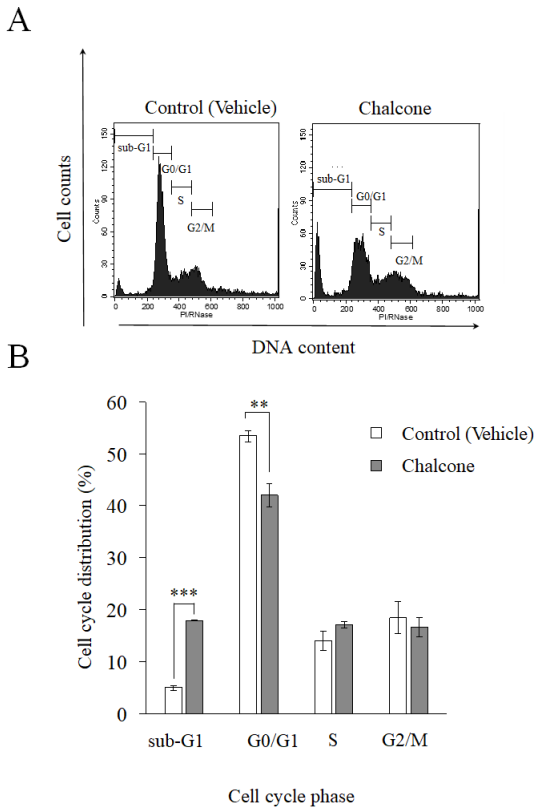

Fig 2. Effect of chalcone on the cell cycle of HeLa CD4$^+$ cells. (A) HeLa CD4$^+$ cells were stained with propidium iodide (PI), the DNA content in the cells was measured by flow cytometry, and the cell cycle phase of each cell was recorded as sub-G1, G0/G1, S, or G2/M. (B) Percentage of cells distributed among different cell cycle phases. Data are expressed as mean ± SD values of three independent experiments. Significant differences between chalcone-treated cells and the control (vehicle) group are labeled (** $P < 0.01$ or *** $P < 0.001$).

3.3. Chalcone induced morphological changes characteristic of apoptosis in HeLa CD4$^+$ cells. PI staining was used to examine chalcone-induced apoptosis. HeLa CD4$^+$ cells were treated with chalcone for 24 h (Fig. 3). Cell shrinkage, apoptotic bodies, nuclear condensation, and nuclear fragmentation, each of which are typical morphological features of apoptosis, were observed. This result was consistent with the results of a study examining the effect of chalcone addition on the cell cycle, which showed an increased percentage of cells with fragmentation of the nuclei in the sub-G1 phase.

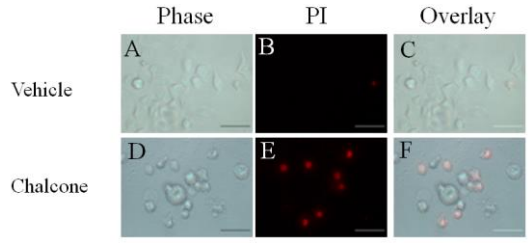

Fig 3. Morphological observation by propidium iodide (PI) staining. Morphology was observed from PI-stained phase contrast images (left), and a fluorescence image (center) and a merge image (right) were thus obtained. (A) to (C) show chalcone-free cells, while (D) to (F) show cells to which 50 μmol/L chalcone was added. (A–F) show cells 24 h after chalcone addition. Morphological change in cells were observed by microscopy. Scale bar, 50 μm.

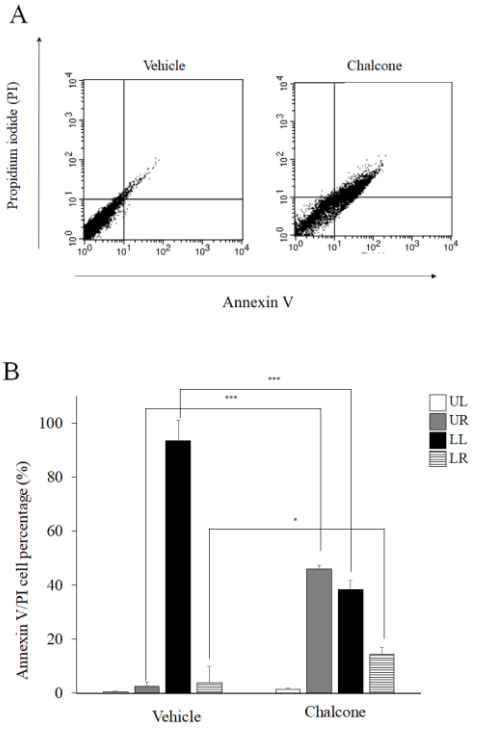

Fig 4. Induction of HeLa CD4$^+$ cell apoptosis by chalcone. (A) Apoptosis rates were determined by flow cytometry analysis using annexin V-FITC/PI double labeling. HeLa CD4$^+$ cells were treated for 24 h in the absence or presence of 50 μmol/L chalcone. (B) Histogram of quantitative analysis of dead (UL), late apoptotic (UR), viable (LL), and early apoptotic (LR) control HeLa CD4$^+$ cells or HeLa CD4$^+$ cells treated with 50 μmol/L chalcone for 24 h. Values are expressed as mean ± SD values of three replicates. * $P < 0.05$ or *** $P < 0.001$ compared with the untreated control (vehicle) group.

3.4. Chalcone induced apoptosis of HeLa CD4$^+$ cells. Using flow cytometry and an annexin V-FITC / PI double labeling assay, we quantified the percentage of apoptotic cells 24 h after the addition of chalcone to HeLa CD4$^+$ cells. Based on the resulting flow cytometry data, each stained cell was classified into one of four groups: (1) viable (LL), (2) early apoptosis (LR), (3) late apoptotic or necrotic (UR), and (4) dead cells (UL). The percentage of late apoptotic cells and early apoptotic cells significantly increased after the 24 h incubation with chalcone (Fig. 4A). While the percentage of late apoptotic or necrotic cells was 3.9 ± 1.3% under control conditions, the apoptosis rate induced by the 24 h incubation with chalcone was significantly increased to more than 11 times higher, at 46.0 ± 8.7% (Fig. 4B).

3.5. Chalcone induced caspase-dependent cell death in HeLa CD4$^+$ cells. We also examined whether caspases are major molecular regulators of cell death. Data are presented as a percentage of chalcone-free controls (Fig. 5). After chalcone treatment, the activity levels of caspase-8, -9, and -3 increased from 9.9 ± 2.0% to 35.5 ± 3.4%, from 9.1

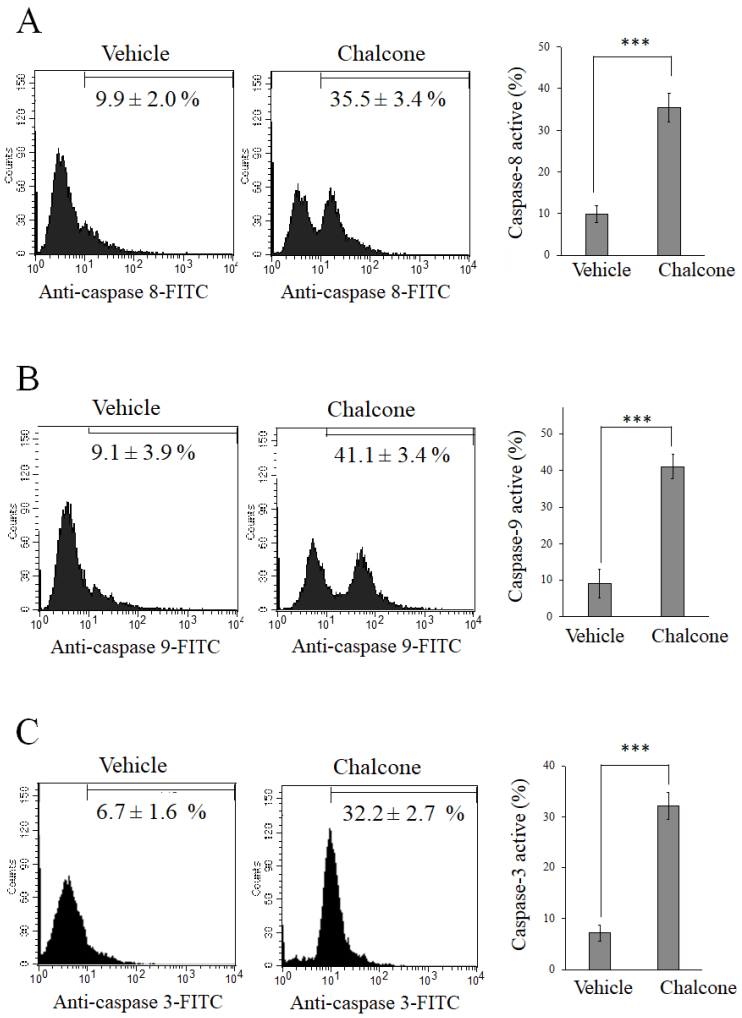

Fig 5. Caspase-8, -9, and -3 activity levels and effects of caspase inhibition on chalcone-treated HeLa CD4$^+$ cells. Caspase-8 (A), -9 (B), and -3 (C) activity was measured by flow cytometry in HeLa CD4$^+$ cells after a 24 h chalcone treatment. The apoptotic cell populations for active caspase-8, caspase-9, and caspase-3 were quantitatively analyzed (left) and graphed (right). Data are represented as mean ± SD values of three experiments. *** $P < 0.001$ compared with the untreated control (vehicle) group.

± 3.9% to 41.1 ± 3.4%, and from 6.7 ± 1.6% to 32.2 ± 2.7%, respectively.

4 Discussion

Among women aged 15 to 44, cervical cancer is the second most common cancer and cancer-related cause of mortality[1)] . Cervical cancer onset and treatment side effects can significantly impact patient QOL[28)] . So, it is important to develop new drugs with few side effects. Apoptosis plays an important role in various diseases, including as a target and side effect of many cancer treatments, and presents an approach to modulating related apoptotic pathways in cancer drug discovery research[29,30)] . Drugs that restore or modulate normal apoptotic pathways allow for the effective treatment of cancers that are dependent on abnormalities in apoptotic pathways[31)] . Accordingly, as a drug identification strategy, it is useful to find anticancer drugs that promote apoptosis[32)] . Ashitaba is a common vegetable and medicinal plant containing many phytochemicals, including the naturally occurring chalcones 4-hydroxydericin, xanthoangelol, and ashitaba chalcone, each of which can be isolated from the plant's roots[11)]. The anticancer activity of synthetic chalcone utilizing the compound's basic structure has also been widely studied[33)] . However, efforts to explore the mechanisms by which the basic structure of chalcone is cytotoxic to cervical cancer cells, and more generally, the anticancer activity of chalcone against cancer cell lines, have been insufficiently examined. Therefore, we aimed to elucidate the mechanism of apoptosis induced by chalcone in HeLa $CD4^+$ cells, a widely researched cervical cancer cell line, and this study was more broadly conducted to provide biochemical evidence for the apoptotic activity of chalcone.

First, the cytotoxicity of chalcone to HeLa $CD4^+$ cells was examined. Chalcone exhibited concentration-dependent cytotoxicity to HeLa $CD4^+$ cells, and the viability of HeLa $CD4^+$ cells was 50% after the 24 h approximately 50 μmol/L chalcone treatment (Fig. 1). Subsequently, cell cycle analysis was performed in order to examine the effect of chalcone on the cell cycle of HeLa $CD4^+$ cells. No significant difference was observed in the percentages of cells in the S phase and the G2/M phase between chalcone-treated cells and control cells. However, significantly more chalcone-supplemented cells were in sub-G1 phase compared to control cells (Fig. 2). Furthermore, in order to confirm whether the effect of chalcone on sub-G1 phase cells was related to apoptosis, HeLa $CD4^+$ cells were subjected to PI staining 24 h after the addition of chalcone, serving as a morphological cell death assay. Cells in the control group exhibited normal morphology (Fig. 3A), but after addition of chalcone, HeLa $CD4^+$ cells exhibited contraction and apoptotic bodies in phase contrast images (Fig. 3D). In the early course of apoptosis, contraction and concentration of cells is observable with an optical microscope[34)]. Cell contraction reduces cell size and increases the density of the cytoplasm, causing the organelles to become more densely packed; pyknosis occurs as a result of chromatin condensation, which is one of the morphological features of apoptosis[35)]. Subsequently, PI staining was conducted to assess changes in the nucleus. The nuclei of cells undergoing apoptosis were examined for nuclear condensation by fluorescence microscopy (Fig. 3E). These results indicated that chalcone prominently induces apoptosis in HeLa $CD4^+$ cells. The fluorescence microscopy analysis of PI stained cells indicated that chalcone is an inducer of cell apoptosis, and the flow cytometric analysis of cells stained with annexin V-FITC and PI revealed the relevance of apoptosis induction. On the surface of apoptotic cells, the normal inward phosphatidylserine of the cell's lipid bilayer migrates and is expressed in the outer layer of the plasma membrane[36)]. Annexin is a

recombinant phosphatidylserine-binding protein that specifically and strongly interacts with phosphatidylserine residues and is therefore used to detect apoptosis[37,38]. In addition, the membrane-impermeable nucleic acid dye propidium iodide (PI) passes through the cell membrane of apoptotic cells that are collapsing[34]. Therefore, double positive results for Annxin V and PI suggest apoptosis. Flow cytometry of apoptotic cells revealed the accumulation of apoptotic cells in the upper right (UR) quadrant after chalcone treatment (Fig. 4). Furthermore, the annexin V-FITC and PI staining results were consistent with each other, confirming that chalcone induced apoptosis in HeLa $CD4^+$ cells. Apoptosis is tightly controlled by anti- and pro-apoptotic proteins and is promoted by various pathways[28]. Apoptotic cells exhibit biochemical modifications such as protein cleavage, protein cross-linking, DNA degradation, and phagocytosis recognition. The proteolytic cascade caspase can activate other caspases, leading to cell death by amplifying the signal transduction pathway of apoptosis[39]. Therefore, to identify the apoptotic pathway induced by chalcone treatment, caspase expression was examined. The protein expression levels of caspase-8, -9, and -3 by HeLa $CD4^+$ cells increased after chalcone treatment (Fig. 5). Induction of apoptosis in HeLa $CD4^+$ cells by chalcone indicates that caspase-3 was activated by an upstream cascade including caspase-8 and caspase-9 activity. Ultimately, this results in the proteolytic activation of caspase-activated DNase, and consequent nuclear fragmentation was induced as shown by cell cycle analysis and PI staining. In this study, we showed that chalcone-induced apoptosis of HeLa $CD4^+$ cells by was due to activation of caspase-3 by the exogenous pathway caspase-8 and the intracellular mitochondrial pathway caspase-9. Chalcone has been suggested to induce apoptosis in cells through both intrinsic and extrinsic pathways. The design of anticancer agents that target the chalcone-induced apoptotic pathway may provide an effective treatment with few side effects. Designing a drug by targeting the chalcone-induced apoptotic pathway as a cancer therapeutic drug might enable the production of a drug that is more effective and has fewer side effects. Natural products are gaining increasing attention due to their potential anti-cancer activity and low intrinsic toxicity. In addition to chalcone, attention has been paid to the anticancer activity of flavonoids. Epigallocatechin gallate (EGCG), which is the main component of green tea polyphenol, has been reported to have anticancer activity against breast cancer[40]. Zan *et al*. reported that EGCG induced apoptosis in breast cancer MCF-7 cells through activation of caspase-9, caspase-3, and poly (ADP-ribose) polymerase-1 cleavage[41]. Also Kwak *et al*. found that EGCG induces apoptosis in human cholangiocarcinoma HuCC-T1 cells through an increase in the apoptosis-promoting proteins Bax, activation of caspase-9 and caspase-3, and release of cytochrome c[42].

In the future, comprehensive elucidation of the effects of chalcones on cancer cells at the DNA and mRNA levels should be a major focus of drug research and development.

Acknowledgments. We would like to thank Ms. S. Mitsutake for helping us with this experiment.

References

1) L. Bruni, L. Barrinuevo-Rosas, G. Albero, B. Serrano, D. Mena, M. Gomez, https://www.hpvcentre.net/statistics/reports/XWX.pdf (**2019**).
2) J. Ferlay, M. Colombet, I. Soerjomataram, C. Mathers, D. M. Parkin, M. Piñeros, A. Znaor, F. Bray F, *Int. J. Cancer*, **2019**, *144*, 1941-1953.
3) T. Papathemelis, S. Knobloch, M. Gerken, A. Scharl, M. Anapolski, A. Ignatov, E. C. Inwald,

O. Ortmann, S. Scharl, M. Klinkhammer-Schalke, *J. Cancer Res. Clin. Oncol*., **2019**, *145*, 1369-1376.

4) A. B. Mutombo, C. Simoens, R. Tozin, J. Bogers, J. P. Van Geertruyden, Y. Jacquemyn, *Syst. Rev*., **2019**, *8*, 132.

5) B.Colagiuri, H. Dhillon, P. N. Butow, J. Jansen, K. Cox, J. Jacquet, *J. Pain Symptom Manage*., **2013**, *46*, 275-281.

6) D. J. Newman, G. M. Cragg, K.M. Snader, *J. Nat. Prod*., **2003**, *66*, 1022-1037.

7) E-M. Suolina, R.N. Buchsbaum, E. Racker, *Cancer Res*., **1975**, *35*, 1865-1872.

8) M. Yoshida, T. Sakai, N. Hosokawa, N. Marui, K. Matsumoto, A. Fujioka, H. Nishino, A. Aoike, *FEBS Lett.*, **1990**, *260*, 10-13.

9) Z. P. Chen, J.B. Schell, C. T. Ho, K. Y. Chen, *Cancer Lett.*, **1998**, *129*, 173-179.

10) J.H. Chung, J.H. Han, E. J. Hwang, J. Y. Seo, K. H. Cho, K. H. Kim, J. I. Youn, H. C. Eun, *FASEB J.*, **2003**, *17*, 1913-1915.

11) T. Okuyama, M. Takata, J. Takayasu, T Hasegawa, H Tokuda, A. Nishino, H Nishino, A. Iwashima , *Planta Med*., **1991**, *57*, 242-246.

12) S. Shibata, *Stem Cells*, **1994**, *12*, 44-52.

13) M. N. Gomes, E. N. Muratov, M. Pereira, J. C. Peixoto, L. P. Rosseto, P. V. L. Cravo, C. H. Andrade, B. J. Neves, *Molecules*, **2017**, *22*, 1210.

14) M. L. Go, X. Wu, X. L. Liu, *Curr. Med. Chem*., **2005**, *12*, 481-499.

15) B. Orlikova, D. Tasdemir, F. Golais, M. Dicato, M. Dieterich, *Genes Nutr.*, **2011**, *6*, 125-147.

16) M. Das and K. Manna, *J. Toxicol.*, **2016**, *2016*, 7651047.

17) J. R. Dimmock, D. W. Elias, M. A. Beazely, N. M. Kandepu, *Curr. Med. Chem*., **1999**, *6*, 1125-1149.

18) K. Tabata, K. Motani, N. Takayanagi, R. Nishimura, S. Asami, Y. Kimura, M. Ukiya, D. Hasegawa, T. Akihisa, T. Suzuki, *Biol. Pharm. Bull*., **2005**, *28*, 1404-1407.

19) Y. Kimura and K. Baba, *Int. J. Cancer*, **2003**, *106*, 429-437.

20) Y. Fu, T. C. Hsieh, J. Guo, J. Kunicki, M. Y. Lee, Z. Darzynkiewicz, J. M. Wu, *Biochem. Biophys. Res. Commun*., **2004**, *322*, 263-270.

21) Y. L. Hsu, P. L. Kuo, L. C. Chiang, C. C. Lin, *Clin. Exp. Pharmacol. Physiol*., **2004**, *31*, 414-418.

22) M. F. Maioral, C. D. N. Bodack, N. M. Stefanes, Á. Bigolin, A. Mascarello , L. D. Chiaradia-Delatorre, R. A. Yunes, R. J. Nunes, M. C. Santos-Silva, *Biochimie*., **2017**, *140*, 48-57.

23) R. Ramirez-Tagle, C. A. Escobar, V. Romero, I. Montorfano, R. Armisén, V. Borgna, E. Jeldes, L. Pizarro, F. Simon, C. Echeverria, *Int. J. Mol. Sci*., **2016**, *17*, 260.

24) X. Bai, Y. Ma, G. Zhang, *Oncol. Rep*., **2015**, *33*, 3085-3092.

25) Y. L. Hsu, P. L. Kuo, W. S. Tzeng, C. C. Lin, *Food Chem. Toxicol*., **2006**, *44*, 704-713.

26) K. H. Shen, J. K. Chang, Y. L. Hsu, P. L. Kuo, *Basic Clin. Pharmacol. Toxicol*., **2007**, *101*, 254-261.

27) E. Szliszka, D. Jaworska, M. Ksek, Z. P. Czuba, W. Król, *Int. J. Mol. Sci*., **2012**, *13*, 15343-15359.

28) J. Jakubowicz, P. Blecharz, P. Skotnicki, M. Reinfuss, T. Walasek, E. Luczynska, *Eur. J. Gynaecol. Oncol*., **2014**, *35*, 393-399.

29) W. Hu and J. J. Kavanagh, *Lancet Oncol*., **2003**, *4*, 721-729.

30) O. Kepp, L. Galluzzi, M. Lipinski, J. Yuan, G. Kroemer, *Nat. Rev. Drug Discov*., **2011**, *10*, 221-237.

31) S. W. Fesik, *Nat. Rev. Cancer*, **2005**, *5*, 876-885.

32) S. Goldar, M. S. Khaniani, S. M. Derakhshan, B. Baradaran, *Asian Pac. J. Cancer Prev*., **2015**, *16*, 2129-2144.

33) M. F. Maioral, P. C. Gaspar, G. G. R. Souza, A. Mascarello, L. D. Chiaradia, M.A. Licínio, A. C.

R. Moraes, R. A. Yunes, R. J. Nunes, M. C. Santos-Silva, *Biochimie*., **2013**, *95*, 866-874.
34) S. Elmore, *Toxicol. Pathol*., **2007**, *35*, 495-516.
35) J. F. Kerr, *Toxicology*, **2002**, *181-182*, 471-474.
36) D. L. Bratton, V. A. Fadok, D. A. Richter, J. M. Kailey, L. A. Guthrie, P. M. Henson, *J. Biol. Chem*., **1997**, *272*, 26159-26165.
37) S. Arur , U. E. Uche, K. Rezaul, M. Fong, V. Scranton, A. E. Cowan, W. Mohler, D. K. Han, *Dev. Cell*, **2003**, *4*, 587-598.
38) E. Bossy-Wetzel and D. R. Green, *Methods Enzymol*., **2000**, *322*, 15-18.
39) G. M. Cohen, *Biochem. J*., **1997**, *326*, 1-16.
40) D. Zhang., H. B. Nichols, M. Troester, J. Cai., J. T. Bensen, D. P. Sandler, *Int. J. Cancer*, **2020**, *147*, 876-886.
41) L. Zan, Q. Chen, L. Zhang, X. Li, *Bioengineered*, **2019**, *10*, 374-382.
42) T. W. Kwak, S.B. Park, H-J. Kim, Y-L. Jeong, D. H. Kang, *Onco Targets Ther*., **2016**, *10*, 137-144.

ISS 実行委員長

羽田　宜弘

第 4 回　ISS（International Student Symposium）の開催と活動成果

去る 2021 年 8 月 29 日（日）に、主催材料技術研究協会による International Student Symposium 2021（ISS2021）を公益財団法人東京応化科学技術振興財団及び東京エレクトロン（株）の助成及び N PO 法人健康福祉工学会の後援を得て、ISS2021 を昨年度と同様オンラインで開催したので、内容について報告をする。

今年度も新型コロナウィルス拡大の影響を受け、オンライン開催を行なった。コロナ禍で教育活動がほとんどの学校でストップしていた時期にも関わらず、ISS に向けて研究や探究活動がされていた高校、大学、大学院の生徒や学生らと教職員及びなど総勢 108 名の参加申し込みがあった。

ISS は、材料技術研究協会が取り組む、「次世代サイエンティストの育成」というテーマを掲げ、専門家の発表する学会という高い敷居を設けず、生徒や学生ら限定の日々の研究、探究成果の発表の機会を創出することと次世代の科学

者を目指す若者らの交流と科学教育に貢献する目的としてスタートし、今年度で 4 年目を迎えた。当日は、口頭発表 9 件、ポスター発表 15 件の大変多くの分野の課題研究や探究活動の発表がされ、他に類を見ない発表の機会となっており、新た価値を創出する上でのヒントになっているものである。

また、ISS では、特に優秀であった発表に対して賞を授与しており、材料技術研究協会の理事らの専門家が各発表の審査にあたり審査基準に基づき厳正なる審査を行い、ゴールド賞，シルバー賞、ブロンズ賞が選出され表彰された。

また開催後のアンケートにおいては以下のような結果を得たので、　併せて報告をする。

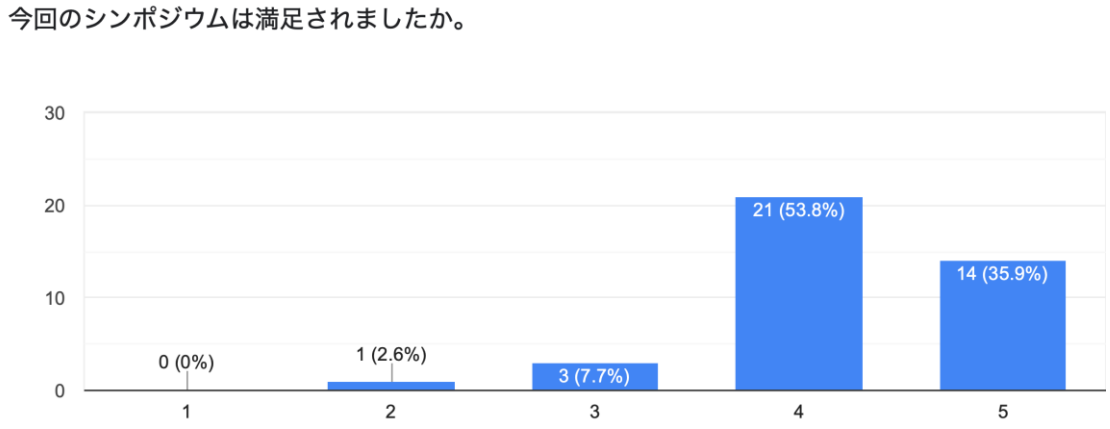

1.　全く満足しなかった　2.満足できなかった。　3. 普通　4. 満足した　5.大変満足

89.7%の参加者が満足または大変満足と答えており，本シンポジウムの高い満足度が示された。

今年度は ZOOM による発表だけではなく、「Ovice」という新しいアプリケーションでの学会会場を設置し、バーチャルで交流ができるように工夫をした。

※参考イメージ

また,ポスター会場は、リアルなポスター会場に近づけるため 3D での空間を制作し、若者が親しみやすい新しい環境での発表会場を用意した。

※参考イメージ

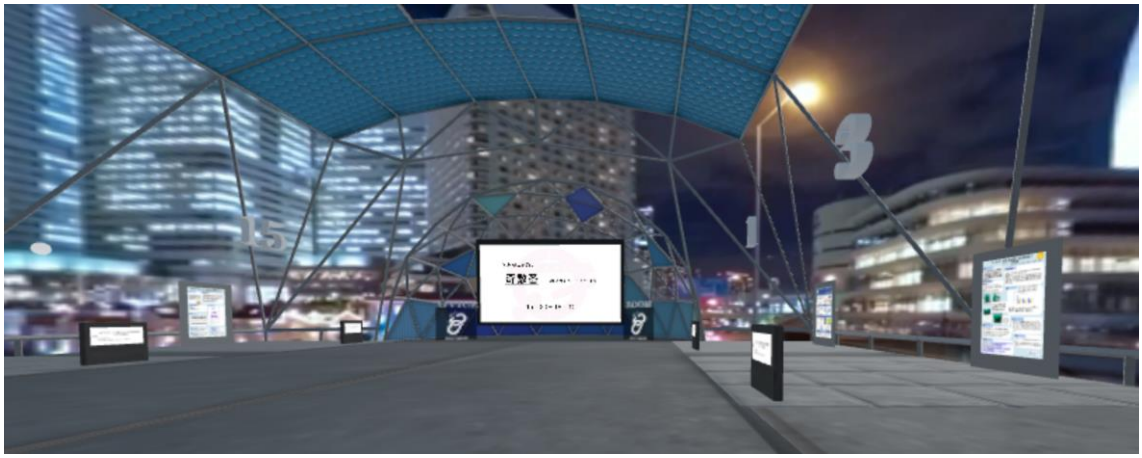

こちらの 3D の会場は、無料のプラットフォームを利用して、作成したもので、会場に多くの人がアクセスすると人数制限がかかるなど、満足のいく形でのポスター発表はできなかったが、ZOOM だけでは難しいオンライン上での学会発表の課題に対してチャレンジし、取り組めたことは参加者からも良かったという声が聞こえた。

次年度についても、工夫や改善をしながら、本事業に取り組んでいきたい。

最後に、この ISS を開催するにあたり、ISS 実行委員の協会理事の皆様、事務局及び助成や後援として多大な協力をいただきました組織の皆様に心からお礼を申し上げます。

MATERIAL TECHNOLOGY 材料技術

昭和62年8月5日第三種郵便物許可　令和３年10月25日発行（隔月25日発行）　第39巻　第５号
定価2,100円